

DISCOVERY AND CHARACTERIZATION OF THE FIRST KNOWN INTERSTELLAR OBJECT

KAREN J. MEECH,¹ ROBERT WERYK,¹ MARCO MICHELI,^{2,3} JAN T. KLEyna,¹ OLIVIER HAINAUT,⁴ ROBERT JEDICKE,¹
RICHARD J. WAINSCOAT,¹ KENNETH C. CHAMBERS,¹ JACQUELINE V. KEANE,¹ ANDREEA PETRIC,¹ LARRY DENNEAU,¹
EUGENE MAGNIER,¹ MARK E. HUBER,¹ HEATHER FLEWELLING,¹ CHRIS WATERS,¹ EVA SCHUNOVA-LILLY,¹ AND
SERGE CHASTEL¹

¹*Institute for Astronomy, 2680 Woodlawn Drive, Honolulu, HI 96822, USA*

²*ESA SSA-NEO Coordination Centre, Largo Galileo Galilei, 1, 00044 Frascati (RM), Italy*

³*INAF - Osservatorio Astronomico di Roma, Via Frascati, 33, 00040 Monte Porzio Catone (RM), Italy*

⁴*European Southern Observatory, Karl-Schwarzschild-Strasse 2, D-85748 Garching bei München, Germany*

(Received November 1, 2017; Revised TBD, 2017; Accepted TBD, 2017)

Submitted to Nature

ABSTRACT

Nature Letters have no abstracts.

Keywords: asteroids: individual (A/2017 U1) — comets: interstellar

1. SUMMARY

Until very recently, all $\sim 750\,000$ known asteroids and comets originated in our own solar system. These small bodies are made of primordial material, and knowledge of their composition, size distribution, and orbital dynamics is essential for understanding the origin and evolution of our solar system. Many decades of asteroid and comet characterization have yielded formation scenarios that explain the mass distribution, chemical abundances and planetary configuration of today’s solar system, but it has remained a mystery how typical our solar system is. On 2017 October 19, the Pan-STARRS1 survey telescope discovered asteroid A/2017 U1, the first object known to originate outside our solar system. Follow-up observations by other observers and subsequent analysis verified the extrasolar trajectory of A/2017 U1 and reveal the object to be asteroidal, with no hint of cometary activity despite an approach within 0.25 au of the Sun after multiple solitary orbits around the galaxy at temperatures that would preserve volatile ices for billions of years. Spectroscopic measurements show that the object’s surface is consistent with comets or organic-rich asteroid surfaces found in our own solar system. Light-curve observations of A/2017 U1 indicate that the object has an extreme oblong shape, with a 10:1 axis ratio and a mean radius of 102 ± 4 m, and given its similar surface composition to solar system asteroids, suggests that such shapes are common during the formation epoch when asteroids are likely to be ejected from their solar systems. The discovery of A/2017 U1 suggests that previous estimates of the density of interstellar objects were pessimistically low. Imminent upgrades to contemporary asteroid survey instruments and improved data processing techniques are likely to produce more interstellar objects in the upcoming years, creating opportunities to interrogate the mineralogical, elemental or isotopic composition of material from other solar systems.

2. OBSERVATIONS

On 2017 October 19 the Pan-STARRS1 telescope system detected an object moving rapidly west at 6.2 degrees per day (Figure 1A). A search of images from the previous nights found the object had also been imaged on October 18. Additional images acquired with the Canada-France-Hawaii Telescope (CFHT) on October

22 confirmed that this object is unique, with the highest known hyperbolic eccentricity of 1.188 ± 0.016^{29} . Data obtained by our team and other researchers between October 14–29 refined its orbital eccentricity to a level of precision that confirms the hyperbolic nature at $\sim 300\sigma$. Designated as A/2017 U1, this object is clearly from outside our solar system (Figure 2).

The October 22 CFHT observations were tracked at the object’s rate of motion and showed no evidence of cometary activity (Figure 1B) in excellent seeing ($0''.5$). A/2017 U1’s point spread function was consistent with a stellar profile with no asymmetry and no coma, implying that it is asteroidal. Additional time-resolved sequences of images at multiple wavelengths on October 25–26 UT with the European Southern Observatory Very Large Telescope, and on October 26–27 UT with the Gemini South Telescope, further strengthened A/2017 U1’s asteroidal identification (Figure 1C). The upper limit for the dust coma brightness (see Methods) is $g > 25.8$ in the wings of the object’s point-spread function (1–2'' from the center), and $g > 29.8 \pm 0.05$ mag/arcsec² at the 5σ level outside the point spread function ($> 5''$ from the center). Using the upper limit to the light that could be scattered by dust we determined that less than 1.7×10^{-3} kg/s of gas could be released from the surface. This is 7–8 orders of magnitude less than a typical long-period comet would produce if there was near-surface water ice (see Methods).

A period search on A/2017 U1’s lightcurve (Figure 3, see Methods) indicates its rotation is $\sim 7.34 \pm 0.06$ hours under the customary assumption that the double-peaked lightcurve is dominated by the shape of the object. No other period gives a satisfactory re-phased lightcurve and the value is not unusual for known objects of this size.

The median magnitude of the object gives it an average radius of ~ 100 m but the very large amplitude of its lightcurve implies that the object is extremely elongated—with an axis ratio of at least 10:1 (see Methods) or that it has large albedo variations or both. A/2017 U1’s red surface color is consistent with the organic-rich surfaces of comets, D-type asteroids, and outer solar system small bodies (Figure 4): its measured colors ($g - r = 0.84 \pm 0.05$, $g - i = 1.15 \pm 0.10$, $g - z = 1.25 \pm 0.10$, $g - Y = 1.60 \pm 0.20$ are consistent with uniform colors over the whole surface of the object; see Methods) provide evidence that A/2017 U1 is compositionally indistinguishable from similar objects in our own solar system despite its curious morphology.

3. DISCUSSION

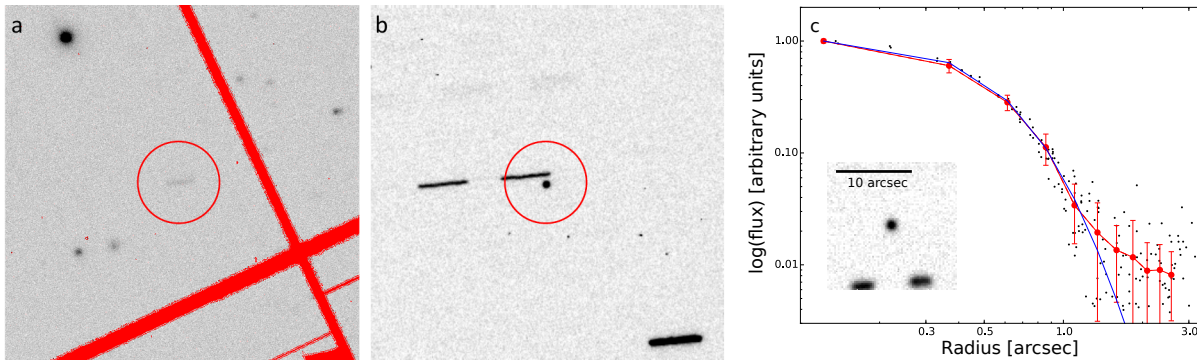


Figure 1. [A] Discovery image of A/2017 U1 from Pan-STARRS1 on 2017 October 19. In this 45 second w_{P1} -band sidereally-tracked image, the object is the trail centered in the circle. Red regions are masked pixels, mostly due to gaps between CCD cells. [B] A/2017 U1 image obtained from CFHT on 2017 October 22, tracked at the object's rate of motion. This composite 180 second w -band image shows no hint of activity although the object was at a heliocentric distance of 1.22 au, just 43 days past perihelion at 0.25 au on 2017 September 09. [C] Deep stacked image combining Gemini and VLT g and r -band data. The red line shows the average flux in the annulus at each radius and the blue line is the Moffat profile²⁶ with a FWHM of $0''.87$.

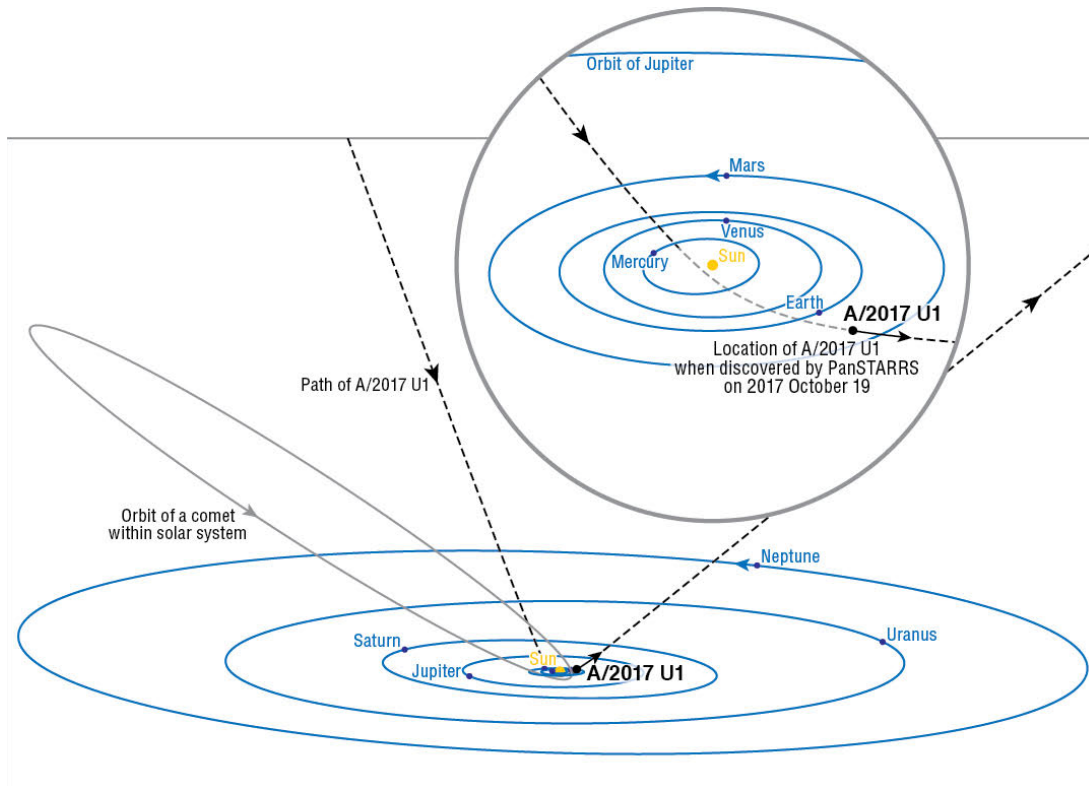


Figure 2. The path of A/2017 U1 through our solar system in comparison to the orbit of a typical Halley-type comet. The inset shows the inner solar system, with the solid line segment along A/2017 U1's trajectory indicating the short window during which it was bright enough to be detected by telescopes on Earth. The path is shown as a lighter shade when the object was below the ecliptic. Credit: Brooks Bays / SOEST Publication Services / UH Institute for Astronomy.

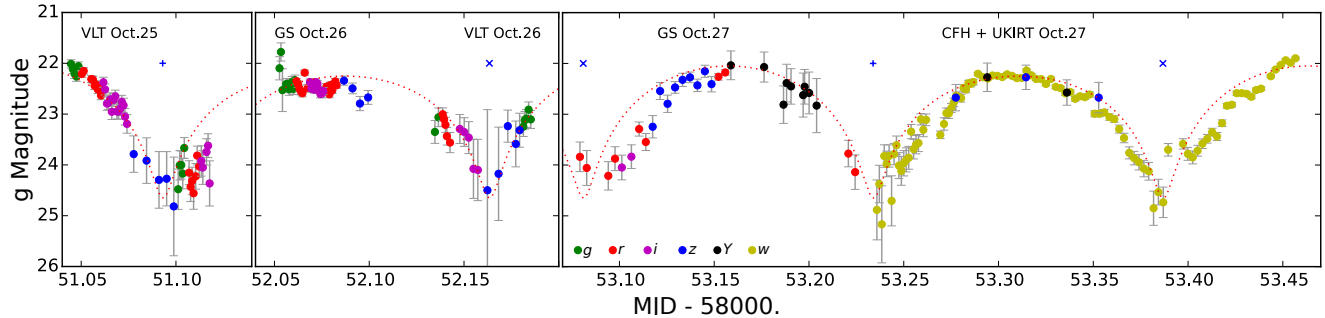


Figure 3. Lightcurve of A/2017 U1. All the magnitudes have been scaled to g -band using the measured colors, and to the geometry of October 25.0. The dotted line corresponds to a 10:1:1 triaxial ellipsoid with a 20% hemispheric variation of albedo, rotating with a 7.34 hour period; the “+” and “X” identify the two minima of the double-peaked lightcurve.

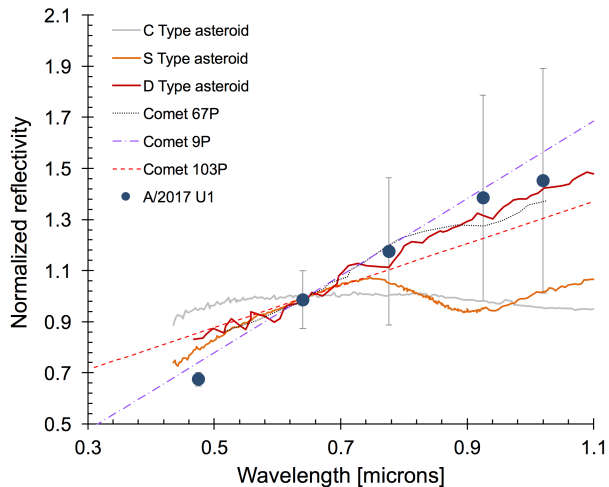


Figure 4. Reflectivity of the surface of A/2017 U1 showing that it is consistent with D-type asteroids and comets. Data are normalized to 1.0 at $0.65 \mu\text{m}$.

The asteroidal nature of A/2017 U1 is surprising given that the predicted ratio²³ of cometary to asteroidal material from contemporary solar system formation models ranges from 200:1 to 10000:1. Indeed, asteroidal objects on long period comet (LPC) orbits in our own solar system have only recently been discovered²³ and are known as Manx-type comets. Most LPCs were originally scattered into the Oort cloud during our solar system’s formation and are now being dislodged and returned to the solar system after ~ 4.6 Gyr of exposure to an interstellar environment, yet most are active objects and are expected to be active for thousands of perihelion passages. Because A/2017 U1 is smaller than most of the known comets it is difficult to compare it directly to comets in our solar system. Given that LPCs retain their volatiles over Gyr time scales and the fact that A/2017 U1 has been at the temperatures of interstellar space for a long time, any ice should have survived for billions of years. However, since no similar sized inactive objects on LPC orbits have been discovered in our

own solar system, and Manx-type comets are rare, it is difficult to reconcile A/2017 U1’s discovery with our current understanding of LPC formation and composition. If the typical ISO is asteroid-like then the ISO number density could be much higher than contemporary limits would suggest.

The highly elongated shape is very unusual. For comparison, strengthless triaxial ellipsoids have a maximum lightcurve amplitude of 0.9 mags and only two other known objects have maximum lightcurve amplitudes > 2.5 mags. Those two objects are much larger than A/2017 U1 and it may be expected that smaller objects are more likely to have more mechanical strength capable of sustaining a highly elongated shape. However, there are no known objects of comparable size in our solar system with lightcurve amplitudes approaching that of A/2017 U1 and it raises the question of why the first known ISO is so unusual.

Many objects that are first detected moving as fast as A/2017 U1 are lost if they are not immediately targeted for more observations. Furthermore, ISOs with high rates of motion may have posted to the Near Earth Object Confirmation Page (NEOCP) but recovery efforts would have targeted incorrect predicted positions assuming they are small, nearby, and with elliptical orbits. In general, one night after discovery an ISO would be located to the west of the predicted position of an NEO with similar motion, and outside the region that is assumed as a realistic uncertainty for regular elliptical orbits. In A/2017 U1’s case the geometry was such that some elliptical solutions overlapped with the true hyperbolic solution and its predicted location on the sky was therefore serendipitously imaged in follow-up observations.

Complicating the ISO discovery rate even more, two-thirds of ISOs that display cometary activity would not rank high enough to post to the NEOCP upon discovery based only upon their apparent rates of motion¹¹. Instead, the detections would have to be identified as un-

usual (cometary) based on their non-stellar point-spread function and then subsequent targeted follow-up observations would allow their identification as ISOs.

The ISO discovery rate could be improved by increasing the survey depth and sky coverage rate. The surveys could also self followup⁸ but this would reduce the NEO discovery rate from which the surveys derive their funding. The ISO detection rate may also be improved with enhanced source detection algorithms for trailed and/or non-stellar sources in images.

It has been suggested² there is a flux of very small ($< 100 \mu\text{m}$) interstellar meteoroids from the debris disk around β -Pictoris. For A/2017 U1, the asymptotic radiant is toward right ascension $18^{\text{h}}44^{\text{m}}$ and declination $+34.5^\circ (\pm 6')$, located near the current position of the Vega debris disk¹⁶ at $18^{\text{h}}36^{\text{m}} +38.8^\circ$. However, the travel time to Earth from the distance of Vega is $\sim 290\,000$ years. Accounting for Vega's proper motion, A/2017 U1 could not have been ejected from the Vega system.

Alternatively, a close encounter between an Oort cloud or Halley-type comet and a small undiscovered nearby planet²⁷ could possibly perturb the smaller object onto a hyperbolic orbit. For such a planet to remain undiscovered for so long, it must be located near the Galactic Plane (which most NEO surveys avoid) and we note that A/2017 U1's radiant has a galactic latitude of $\sim 16^\circ$. It is also possible that a more distant, larger undiscovered planet in our own solar system could have perturbed A/2017 U1 into an unbound orbit. Batygin & Brown³ suggest the location of a distant $\sim 10M_\oplus$ planet many hundreds of AU from the Sun, but the best estimate of its orbital plane does not contain the radiant direction of A/2017 U1. Although we believe it unlikely that an undiscovered planet could have produced the motion of A/2017 U1, we cannot yet rule it out. A deep search for distant planets in the radiant direction of A/2017 U1 would help to confirm or reject this possibility.

The discovery of an interstellar object adds a new component, albeit small, to the Earth impact risk: impact from an interstellar object would be far more energetic than from a solar system object with similar mass, due to the larger impact speed. Meteorites resulting from such an impact would show an age inconsistent with that of our solar system.

The incoming velocity of A/2017 U1 in the Local Standard of Rest is ($U = 11.3, V = -22.3, W = -7.6$ km s⁻¹). This is comparable with the mean and standard deviation of the motion of stars in the local solar neighborhood¹². The implication is that A/2017 U1 was orbiting the galactic center in a manner close to the mean motion of the solar neighborhood and has no

greater relationship with the stars of the solar neighborhood than they have with each other, which is effectively none. A/2017 U1 has likely orbited the galaxy multiple times and its system of origin could today be on the other side of the galaxy. This also suggests that the solar perihelion of A/2017 U1 was its first close encounter with a star and the first opportunity to warm any volatiles.

A population of interstellar asteroids could arise from scattering events in their host system when major planets migrated through strong resonances and ejected objects with more mature processed material than those in their Oort cloud. The A/2017 U1 discovery suggests there are likely additional ISOs in our solar system at any given time and raises the tantalizing prospect of many more future ISO discoveries. These objects will enable the measurement of elemental abundances in other solar systems and test planetary formation theories. Calculating a formal interstellar influx number density and predicting their future discovery rate by existing and planned sky surveys from the single A/2017 U1 discovery is beyond the scope of this work and would require a detailed simulation of the surveys' ISO detection efficiency¹¹, which is complicated by regular improvements to the surveys' operations. Indeed, it is likely that the A/2017 U1 discovery was made possible by recent improvements to the Pan-STARRS1 detection pipeline. Our estimates suggest that there is always about one ISO of about 250 m diameter (assuming a 4% albedo) within 1 au of the Sun, that is, interior to Earth's orbit (see Methods).

4. METHODS

Discovery and Orbit Determination – The October 19 detection of A/2017 U1 by the Pan-STARRS1 telescope²⁹ used four sidereally tracked w_{P1} -band images obtained in poor seeing conditions (with a stellar FWHM of $2''.2$) during normal survey observations for near-Earth objects²⁸. Two additional w_{P1} -band pre-discovery images from 2017 October 18 were then identified in images with stellar FWHMs of $1''.8$ and $2''.4$. It was not possible to detect low-level cometary activity in these images due to poor seeing and the object being trailed.

Both elliptical and parabolic heliocentric orbits gave atypically large fit residuals when additional astrometry beyond the original detections were included. Follow-up observations with the ESA Optical Ground Station also did not fit and were blocked by the Minor Planet Center (MPC) automated routines as suspected outliers. Our investigation revealed that this object could be explained using a hyperbolic orbit with a preliminary ec-

Table 1. Orbital elements of A/2017 U1 based on observations collected between 2017 October 14–29.

Element	Heliocentric	Barycentric [†]
v_∞ (km/s)	-	26.15 ± 0.05
q (au)	0.25400 ± 0.00026	0.25083 ± 0.00026
e	1.1960 ± 0.0007	1.1933 ± 0.0007
i (deg)	122.561 ± 0.024	122.608 ± 0.024
Ω (deg)	24.6049 ± 0.0010	24.2563 ± 0.0010
ω (deg)	241.46 ± 0.05	241.47 ± 0.05
T	2017-09-09.465	2017-09-09.094
	± 0.005	± 0.005
Epoch	2017-09-09.0	1838-01-01.0

[†]The barycentric elements account for periodic terms connected with the motion of the Sun around the barycenter. The elements were integrated backwards in time until the object was 1000 au from the Sun to remove any possible effects from close encounters during the incoming trajectory. The time-of-passage at pericenter (T) should be interpreted as peribarion in this case.

centricity of $e \sim 1.13$, the largest ever recorded (the next largest being comet Bowell at $e = 1.057$ due to a Jupiter encounter). A/2017 U1 was first classified as an Aten-type object ($a=0.74$ au, $e=0.449$, $i=10^\circ$) when it was posted to the Near-Earth Object Confirmation Page (NEOCP). The Aten-type orbit induced a 5 arc minute error in its predicted location 24 hours later and increased to 34 arc minutes after 48 hours. It was later classified as a Halley-family comet when the Minor Planet Center revised the orbit to ($a=50$ au, $e=0.997$, $i=107^\circ$) after including the Catalina Sky Survey observations on October 20 and the ephemeris error for our pre-discovery observations decreased from 34 to 0.5 arc minutes. The object’s orbit was seen to be clearly hyperbolic after the arc was extended to October 22 by our CFHT observations. With additional Canada-France-Hawaii Telescope astrometry on 2017 October 22 UT (Figure 1B) the eccentricity was revised to $e = 1.188 \pm 0.016$. With a total of 118 observations (ten of which were rejected as outliers) A/2017 U1’s orbital eccentricity is now securely hyperbolic at the $\sim 300\sigma$ confidence level, having a barycentric eccentricity of $e = 1.1933 \pm 0.0007$ (Table 1). The two most significant planetary close approaches were with the Earth (0.16 au ~ 16 Hill radii) and Jupiter (4.82 au ~ 14 Hill radii) but even they are too distant to significantly perturb A/2017 U1 during its approach towards the Sun (nevertheless, the corresponding perturbations have all been modeled in the discussion presented here).

Telescope Observations

Pan-STARRS1—The Panoramic Survey Telescope and Rapid Response System⁵) is a wide field astronomical imaging and data processing facility, having a 3° field of view with $0''.25$ pixels. The data are processed to remove instrumental artifacts, and most objects are automatically detected and photometrically and astrometrically calibrated^{20,21,8}. Fast moving objects that leave trails on the image, like A/2017 U1, must be remeasured before submission to the MPC.

CFHT—For these observations we used the MegaCam wide-field imager, an array of forty 2048×4612 pixel CCDs with a plate scale of $0''.187$ per pixel and a 1.1 square degree FOV. The data were obtained using queue service observing and processed to remove the instrumental signature through the Elixir pipeline¹⁹. Three 60-second exposures were obtained on 2017 October 22 UT using a wide *gri*-band filter with FWHM of $0''.5$ seeing. The exposures were tracked at the predicted motion of the object and obtained in excellent conditions (Fig. 1b). The immediate area surrounding the object was searched for faint companions with similar motion but none were found. A series of MegaCam observations were also obtained on 2017 October 27 UT using the wide *gri*-band filter to obtain a light curve. Integration times were initially 70 seconds but were increased to 180 seconds to improve the SNR. A six-day old moon increased the sky background slightly during the first part of this sequence. The weather during the period October 23–26 on Maunakea was poor and no observations could be obtained.

Gemini South Telescope—We were awarded 3.5 h of Director’s Discretionary (DD) time for rapid observations of a target of opportunity. Data were obtained using the Gemini Multi-Object Spectrograph (GMOS) in imaging mode that uses three $\sim 2048 \times 4176$ Hamamatsu chips. The data were obtained through Sloan Digital Sky Survey (SDSS) filters using queue service observing. The detector was read out with pixels binned 2×2 with slow read (read noise= $3.98 e^-$) and low gain ($1.83 e^-/\text{ADU}$). Exposures were kept to 30 s to minimize trailing.

VLT—Observations were performed at the ESO VLT UT1 on Paranal, Chile, using DD time, tracking the object with short exposures (30 s) to minimize trailing of the stars. We used the FORS2¹ instrument and the g-HIGH+115, R-SPECIAL+76, I-BESS+77, and z-Gunn+78 filters with the “red” CCD, a $2k \times 4k$ MIT de-

telescope. The pixels were read-binned 2×2 resulting in an image scale of $0''.25/\text{pix}$.

United Kingdom Infrared Telescope—The data were taken in 30 s frames while tracking non-sidereally according to the A/2017 U1 ephemeris. Alternating blocks in z and Y band were detrended, registered, and stacked manually.

Visual-band CCD Data Reduction—We reduced all visual-band CCD data using custom code for bias subtraction and flat-fielding to establish a uniform detector response. We fit world coordinates (RA and Dec) using reference stars from the SDSS and 2MASS catalogs, and computed a photometric zero point for each image using stars from the PS1 3π survey⁵. Finally, we measured A/2017 U1’s apparent magnitude by summing the flux inside a $4''$ diameter aperture placed at the adjusted ephemeris location and correcting for the zero point.

Solving for the rotation period and colors—The lightcurve data were first corrected for the observing geometry to normalize the heliocentric and geocentric distances to those of October 25.0 and preliminary color corrections were applied to all the data points. An initial rotation period was then determined using the Phase Dispersion Minimization (PDM) technique²⁵. Then the color indexes ($g-r$, $g-i$, $g-z$, $g-Y$) were included in the PDM to minimize the dispersion between the lightcurve segments to obtain the final period and colors.

We estimated the uncertainty on the period and colors by individually “scanning” through each value. The phased lightcurve for the values at the limit of the interval of confidence were visually checked to be “almost but not quite as good” as the best fit. Rotation periods were scanned in the range from 2 to 20 h to ensure that no other period could reproduce the observations. In particular, the half-period of ~ 3.65 h fails to produce a satisfactory single-peaked phased curve (which would be difficult to explain physically). A period of 11.0 h is marginally acceptable with the PDM metric but produces a 3-peaked lightcurve.

Shape and size—The light curve of a triaxial ellipsoid⁹ with axis ratio $a > b > c$ was fit to A/2017 U1’s lightcurve. As the geometry of the rotation axis is unknown, the aspect angle (between the line-of-sight and the rotation axis) was set to the most probable value of 90° , and results in a lower limit on the elongation. Asteroids usually rotate on their shortest axis, c , for stability. The fit yields an axis ratio of 10:1: c with large uncertainties (Figure 3), c is unconstrained by the lightcurve. We accounted for a small asymmetry between the lightcurve maxima with a periodic signal of 0.2 mag half-amplitude intended to represent a hemi-

spherical relative albedo variation of 20%. Since the albedo and geometric cross-section are degenerate this interpretation is not strong. The resulting model is not unique but is useful to guide the eye. It is clear that A/2017 U1’s lightcurve has systematic deviations with respect to the fit ellipsoid and these likely correspond to large areas where the object is flat or concave (flat and concave cannot be distinguished by the lightcurve as they produce the same cross-section). A roughly spherical object with a hemispheric albedo variation of a factor of 10 could also reproduce the lightcurve but this is unlikely based on our current understanding of the surfaces of most asteroids in our solar system and the absence of any sign of volatiles. Finally, the value of c is undetermined: if the constraint that the asteroid rotates on its smallest axis is relaxed then c could have any value without affecting the lightcurve.

The brightest $g = 22.15$ and faintest $g = 24.65$ lightcurve values show a range of 2.5 magnitudes which implies a 10:1 axis ratio for 2 sides of the ellipsoid. The median g magnitude can be converted to an absolute magnitude of $H_V = 22.4$ (in the H-G asteroid photometric system) after accounting for A/2017 U1’s colors. Using a cometary albedo of $p = 0.04$ and yields an effective radius of 102 ± 4 m (the uncertainties are based only on the magnitude uncertainties). It is meaningless to convert the brightest and faintest magnitudes into linear dimensions because a/c is not constrained.

Assessment of lack of activity—In order to reach the faintest possible surface-brightness, a stack of the g and r images from Gemini and VLT was produced, totaling 1920 s exposure time. By coincidence, the photometric zero points of these two filters are virtually equal, with $ZP_g = ZP_r = 27.98$ (for adu/s/pix). The profile of the object was estimated by averaging its flux in annuli. A Moffat function²⁶ was adjusted to an average profile, resulting in $\alpha = 1''.1$ that corresponds to a FWHM of $0''.87$. The individual pixels and profiles are displayed in Fig. 3. The Moffat profile represents the object’s profile well out to $\sim 2''$, where the sky noise dominates. We assume that *all* the flux difference between the object profile and the Moffat profile corresponds to a coma; this gives $g_{\text{coma}} = 25.8$ for the ring between 1 and $2''$ (to be compared to $g_{\text{A/2017U1}} = 22.5$). This magnitude can be converted into a total diffusing area of dust grains. Assuming an albedo of 0.04/0.2, a bulk density of 1000 or 3000 kg/m^3 (typical values for fluffy and compact cometary grain densities seen from the Rosetta mission¹⁴), and a grain radius $a = 1 \mu\text{m}$, up to 0.5/0.3 kg of dust could be present around in the direct vicinity of the object. Computing a water ice thermal sublimation model shows that the maximum dust production for 1

μm grains that can be sustained and remain below the coma detection limits above is 1.668×10^{-3} kg/s, which corresponds to the order of a few kg within the aperture.

At larger radii from the object, any (not visible) coma would be fainter than the noise background, which is $n = 0.147 \pm 0.005$ adu/s/pix in $0''.25$ pixels. The 3σ (5σ) limits correspond to surface brightnesses of $g = r = 30.4(29.8) \pm 0.05$ mag arcsec $^{-2}$. Using the same assumptions as above, up to 13/8 g (8/4 g), at the 3 (5σ) level of comet/asteroidal dust per pixel could be present. In the $2-2''.5$ annulus (covering ~ 100 pixels), this could represent up to 1 kg.

Estimating the interstellar object number density–

We estimate the ISO number density (ρ_{IS}), i.e. the spatial number density of ISOs far from the influence of any stars, by scaling from earlier upper confidence limits¹¹. They calculated a 90% upper confidence limit on ρ_{IS} of 2.4×10^{-2} au $^{-3}$ for inactive (asteroidal) objects with $H < 19$ assuming an albedo of $p_V = 0.04$ typical of cometary nuclei (corresponding roughly to objects with diameters > 0.5 km diameter). Their limit was based on the lack of discovery of any ISOs during ~ 18 integrated years of surveying using the Pan-STARRS1⁵ and Catalina Sky Surveys⁶. Those surveys subsequently acquired another ~ 12 years of data, so we normalize the survey time based on the discovery rate of $H < 22$ NEOs¹ during and subse-

quent to the original time period. Due to surveying, hardware, and software improvements, the surveys have since discovered roughly 1930 NEOs with $H < 22$ compared to about 1740 objects during the original study. We extrapolate from the $H < 19$ (> 0.5 km diameter) size to $H < 22$ using the size-frequency distribution (SFD) for a self-similar collisional cascade¹⁰ of $N(< H) \propto 10^{0.5H}$ as this SFD is broadly representative of most small body populations in the solar system in this size range¹⁷. Finally, we account for the decreased survey depth (geocentric distance) for objects with $H = 19$ and $H = 22$ because the Pan-STARRS1 system with a V -band limiting magnitude⁸ of ~ 21.7 can detect objects of these absolute magnitudes out to geocentric distances of ~ 1.4 au and ~ 0.55 au respectively. Assuming that most ISOs are inactive, asteroid-like, objects similar to A/2017 U1, the interstellar ISO number density of $\rho_{IS}(H < 19) \sim 0.003$ au $^{-3}$ is surprisingly close to earlier upper confidence limits¹¹. Scaling down in size to $H = 22$, comparable to A/2017 U1, and accounting for the $3\times$ density enhancement due to the Sun's gravity¹¹, suggests that there is always about one ISO with $H < 22$ (about 250 meters diameter assuming $p_V = 0.04$) closer to the Sun than 1 au. i.e. interior to Earth's orbit.

Code availability–

Data availability–

REFERENCES

- [1] Appenzeller, I. et al. Successful commissioning of FORS1 - the first optical instrument on the VLT. *The Messenger* **94**, 1-6 (1998).
- [2] Baggaley, W. J. Advanced Meteor Orbit Radar observations of interstellar meteoroids. *J. Geophys. Res.* **105**, 10353-10362 (2000).
- [3] Batygin, K., & Brown, M. E. Evidence for a distant giant planet in the solar system. *AJ* **151**, 22-33 (2016).
- [4] Bertin, E., & Arnouts, S. SExtractor: Software for source extraction. *A&AS* **117**, 393-404 (1996).
- [5] Chambers, K. C., et al. The Pan-STARRS1 Surveys. Preprint at <https://arxiv.org/abs/1612.05560> (2016).
- [6] Christensen, E., et al. The Catalina Sky Survey: Current and future work. AAS/DPS Meeting #44, #210.13 (2012).
- [7] Cook, N. V., Ragozzine, D., Granvik, M., Stephens, D. C. Realistic detectability of close interstellar comets. *ApJ* **825**, 51-66 (2016).
- [8] Denneau, L., et al. The Pan-STARRS moving object processing system. *PASP* **125**, 357-395 (2013).
- [9] Detal, A., et al. Pole, albedo and shape of the minor planets 624 Hektor and 43 Ariadne: Two tests for comparing four different pole determination methods. *A&A* **281**, 269-280 (1994).
- [10] Dohnanyi, J. S. Collisional model of asteroids and their debris. *JGR* **74**, 2531-2554 (1969).
- [11] Engelhardt, T., et al. An observational upper limit on the interstellar number density of asteroids and comets. *AJ* **153**, 133 (2017).
- [12] Francis, C., Anderson, E. 2009. Calculation of the local standard of rest from 20 574 local stars in the new Hipparcos reduction with known radial velocities. *New Astronomy* **14**, 615-629.
- [13] Fukugita, M., et al. The Sloan Digital Sky Survey Photometric System. *AJ* **111**, 1748-1756 (1996).

¹ <http://www.minorplanetcenter.net/iau/lists/YearlyBreakdown.html> Rostt

- [14]Fulle, M., and 40 colleagues 2015. Density and Charge of Pristine Fluffy Particles from Comet 67P/Churyumov-Gerasimenko. *The Astrophysical Journal* 802, L12.
- [15]Grav, T., et al. The Pan-STARRS synthetic solar system model: A tool for testing and efficiency determination of the moving object processing system. *PASP* **123**, 423-447 (2011).
- [16]Holland, W.S., et al. Submillimetre images of dusty debris around nearby stars. *Nature* **392**, 788-791 (1998).
- [17]Jedicke, R., Larsen, J., & Spahr, T. Observational selection effects in asteroid surveys. *Asteroids III* 71-87 (2002).
- [18]Jewitt, D. Project Pan-STARRS and the outer solar system. *Earth Moon and Planets* **92**, 465-476 (2003).
- [19]Magnier, E. A., & Cuillandre, J.-C. The Elixir System: Data characterization and calibration at the Canada-France-Hawaii telescope. *PASP* **116**, 449-464 (2004).
- [20]Magnier, E. A., et al. Pan-STARRS photometric and astrometric calibration. Preprint at <https://arxiv.org/abs/1612.05242> (2016).
- [21]Magnier, E. A., et al. Pan-STARRS pixel analysis: source detection and characterization. Preprint at <https://arxiv.org/abs/1612.05244> (2016).
- [22]McGlynn, T. A., & Chapman, R. D. On the nondetection of extrasolar comets. *ApJ* **346**, L105-L108 (1989).
- [23]Meech, K. J., et al. Inner solar system material discovered in the Oort cloud. *Science Advances* **2**, e1600038 (2016).
- [24]Moro-Martín, A., Turner, E. L., & Loeb, A. Will the Large Synoptic Survey Telescope detect extra-solar planetesimals entering the solar system?. *ApJ* **704**, 733-742 (2009).
- [25]Stellingwerf, R. F. Period determination using phase dispersion minimization. *ApJ* **224**, 953-960 (1978).
- [26]Trujillo, I., Aguerri, J. A. L., Cepa, J., Gutiérrez, C. M. The effects of seeing on Sérsic profiles - II. The Moffat PSF. *Mon. Not. Astron. Soc.* **328**, 977-985 (2001).
- [27]Volk, K. & Malhotra, R. The curiously warped mean plane of the Kuiper Belt. *AJ* **154**, 62-77 (2017).
- [28]Wainscoat, R. J., et al. The Pan-STARRS search for near Earth objects. *IAU Symposium* **318**, 293-298 (2016).
- [29]Williams, G.V. MPEC 2017-U181: COMET C/2017 U1 (PANSTARRS). <http://www.minorplanetcenter.net/mpec/K17/K17UI1.html> (2017).

Supplementary Information is linked to the online version of the paper at www.nature.com/nature.

Acknowledgements Pan-STARRS1 is supported by the National Aeronautics and Space Administration under grant NNX14AM74G issued through the SSO Near Earth Object Observations Program, RJW Principal Investigator. KJM, JTK, and JVK acknowledge support through awards from the National Science Foundation AST1413736 and AST1617015.

Based in part on observations collected at the European Organisation for Astronomical Research in the Southern Hemisphere under ESO programme 2100.C-5008(A). Also based in part on observations obtained under program GS-2017B-DD-7 at the Gemini Observatory, which is operated by the Association of Universities for Research in Astronomy, Inc., under a cooperative agreement with the NSF on behalf of the Gemini partnership: the National Science Foundation (United States), the National Research Council (Canada), CONICYT (Chile), Ministerio de Ciencia, Tecnología e Innovación Productiva (Argentina), and Ministério da Ciência, Tecnologia e Inovação (Brazil). Based also in part on observations obtained with MegaPrime/MegaCam, a joint project of CFHT and CEA/DAPNIA, at the Canada-France-Hawaii Telescope (CFHT) which is operated by the National Research Council (NRC) of Canada, the Institut National des Sciences de l'Université of the Centre National de la Recherche Scientifique (CNRS) of France, and the University of Hawaii.

We thank all of the directors who rapidly evaluated the requests for telescope time and who facilitated the immediate execution of the programs on the telescopes: Laura Ferrarese (Gemini Observatory), Rob Ivison (ESO), Doug Simons (CFHT), and Robert McLaren (UKIRT). We also thank all of the queue operators and support staff who made the data immediately available to the team. We thank Kanoa Withington for the rapid processing of the CFHT data, Sidik Isani for help with non-sidereal guiding and Watson Varricatt and Mike Irwin with WFCAM non-sidereal scheduling. Finally, we thank the follow-up observers for their confirming astrometry.

Author contributions K.J.M. led the team after discovery including securing the telescope time to characterize the object, helping with observing preparation and data acquisition, data reduction, analysis, and writing. R.W. discovered A/2017 U1 in the Pan-STARRS data and, along with M.M., realized its importance as an object on a hyperbolic orbit. He also contributed to the analysis and writing. M.M. contributed to the realization of the importance of this object, obtained, reduced, and reported the astrometric measurements, integrated the orbit backwards to determine the asymptote, and developed the optimum strategy for future astrometry. He also helped with observing preparation and writing. J.T.K. performed all of the photometry, requiring the development of some new pipeline software, and contributed to other analysis and writing. O.R.H. helped secure the VLT time, prepared the VLT phase II program, did the initial data processing, and developed the rotational lightcurve-color solution. He also contributed to other analysis and writing. R.J. contributed to the analysis, calculated the ISO spatial number density, and made a major contribution to writing the manuscript. R.J.W. contributed to the discovery, obtained early CFHT observations showing asteroidal nature, alerted K.J.M. to the need for mobilization and contributed to the writing. He also secured CFHT telescope time, prepared light curve observations on CFHT, and participated in the interpretation of the data. K.C.C. contributed to the writing and UKIRT photometry and calculation of motion with respect to LSR. J.V.K. prepared the Gemini phase II program, and oversaw the observations, and contributed to the manuscript. A.P. helped with the CFHT mosaic reductions. L.D. Contributed to writing the paper. E.A.M. led the team that developed the PS1 image processing system, contributed Keck 10 m telescope time, and assisted with observing. M.E.H. supports the daily downloads for moving objects. H.F., C.W., and M.E.H. support the IPP system which makes the Pan-STARRS system possible. E.S.L. is part of the team that examines the daily data. S.C. writes and maintains software for extraction of moving objects from the PS1 data.

Author information Reprints and permissions information is available at www.nature.com/reprints. The authors declare no competing financial interests. Correspondence and requests for materials should be addressed to K.J.M. (meech@ifa.hawaii.edu).